

# Long-term trends in nitrogen oxides concentrations and on-road vehicle emission factors in Copenhagen, London and Stockholm

Krecl, Patricia; Harrison, Roy M.; Johansson, Christer; Targino, Admir Créso; Beddows, David C.; Ellermann, Thomas; Lara, Camila; Ketzel, Matthias

DOI:

[10.1016/j.envpol.2021.118105](https://doi.org/10.1016/j.envpol.2021.118105)

License:

Creative Commons: Attribution-NonCommercial-NoDerivs (CC BY-NC-ND)

*Document Version*

Peer reviewed version

*Citation for published version (Harvard):*

Krecl, P, Harrison, RM, Johansson, C, Targino, AC, Beddows, DC, Ellermann, T, Lara, C & Ketzel, M 2021, 'Long-term trends in nitrogen oxides concentrations and on-road vehicle emission factors in Copenhagen, London and Stockholm', *Environmental Pollution*, vol. 290, 118105. <https://doi.org/10.1016/j.envpol.2021.118105>

[Link to publication on Research at Birmingham portal](#)

## General rights

Unless a licence is specified above, all rights (including copyright and moral rights) in this document are retained by the authors and/or the copyright holders. The express permission of the copyright holder must be obtained for any use of this material other than for purposes permitted by law.

- Users may freely distribute the URL that is used to identify this publication.
- Users may download and/or print one copy of the publication from the University of Birmingham research portal for the purpose of private study or non-commercial research.
- User may use extracts from the document in line with the concept of 'fair dealing' under the Copyright, Designs and Patents Act 1988 (?)
- Users may not further distribute the material nor use it for the purposes of commercial gain.

Where a licence is displayed above, please note the terms and conditions of the licence govern your use of this document.

When citing, please reference the published version.

## Take down policy

While the University of Birmingham exercises care and attention in making items available there are rare occasions when an item has been uploaded in error or has been deemed to be commercially or otherwise sensitive.

If you believe that this is the case for this document, please contact [UBIRA@lists.bham.ac.uk](mailto:UBIRA@lists.bham.ac.uk) providing details and we will remove access to the work immediately and investigate.

1 **Long-term trends in nitrogen oxides concentrations and on-road vehicle emission factors in**  
2 **Copenhagen, London and Stockholm**

3

4 Patricia Krecl<sup>a,\*</sup>, Roy M. Harrison<sup>b,c</sup>, Christer Johansson<sup>d</sup>, Admir C. Targino<sup>a</sup>, David C. Beddows<sup>b</sup>,  
5 Thomas Ellermann<sup>e</sup>, Camila Lara<sup>a</sup>, and Matthias Ketzel<sup>e,f</sup>

6

7 <sup>a</sup>Graduate Program in Environmental Engineering, Federal University of Technology, Av. Pioneiros  
8 3131, 86036-370, Londrina, PR, Brazil

9 <sup>b</sup>School of Geography, Earth and Environmental Sciences, University of Birmingham, Edgbaston,  
10 Birmingham, B15 2TT, United Kingdom

11 <sup>c</sup>Department of Environmental Sciences / Center of Excellence in Environmental Studies, King  
12 Abdulaziz University, PO Box 80203, Jeddah, 21589, Saudi Arabia

13 <sup>d</sup>Department of Environmental Science, Stockholm University, Svante Arrhenius väg 8, 106 91,  
14 Stockholm, Sweden

15 <sup>e</sup>Department of Environmental Science, Aarhus University, Frederiksborgvej 399, DK-4000, Roskilde,  
16 Denmark

17 <sup>f</sup>Global Centre for Clean Air Research (GCARE), University of Surrey, Guildford GU2 7XH, United  
18 Kingdom

19

20

21

22 \*Corresponding author:

23 E-mail: patriciak@utfpr.edu.br

24 **Abstract**

25 Road transport is the main anthropogenic source of NO<sub>x</sub> in Europe, affecting human health and  
26 ecosystems. Thus, mitigation policies have been implemented to reduce on-road vehicle emissions,  
27 particularly through the Euro standard limits. To evaluate the effectiveness of these policies, we  
28 calculated NO<sub>2</sub> and NO<sub>x</sub> concentration trends using air quality and meteorological measurements  
29 conducted in three European cities over 26 years. These data were also employed to estimate the trends  
30 in NO<sub>x</sub> emission factors (EF<sub>NO<sub>x</sub></sub>, based on inverse dispersion modeling) and NO<sub>2</sub>:NO<sub>x</sub> emission ratios  
31 for the vehicle fleets under real-world driving conditions. In the period 1998-2017, Copenhagen and  
32 Stockholm showed large reductions in both the urban background NO<sub>x</sub> concentrations (-2.1 and -2.6 %  
33 yr<sup>-1</sup>, respectively) and EF<sub>NO<sub>x</sub></sub> at curbside sites (68 and 43%, respectively), proving the success of the Euro  
34 standards in diminishing NO<sub>x</sub> emissions. London presented a modest decrease in urban background NO<sub>x</sub>  
35 concentrations (-1.3% yr<sup>-1</sup>), while EF<sub>NO<sub>x</sub></sub> remained rather constant at the curbside site (Marylebone Road)  
36 due to the increase in public bus traffic. NO<sub>2</sub> primary emissions –that are not regulated– increased until  
37 2008-2010, which also reflected in the ambient concentrations. This increase was associated with a strong  
38 dieselization process and the introduction of new after-treatment technologies that targeted the emission  
39 reduction of other species (e.g., greenhouse gases or particulate matter). Thus, while regulations on  
40 ambient concentrations of specific species have positive effects on human health, the overall outcomes  
41 should be considered before widely adopting them. Emission inventories for the on-road transportation  
42 sector should include EF<sub>NO<sub>x</sub></sub> derived from real-world measurements, particularly in urban settings.

43

44

45

46 **Key words:** NO<sub>x</sub>; air quality in Europe; OSPM model; road transport; dieselization.

## 47 **1. Introduction**

48 Road transport is the main anthropogenic source of nitrogen oxides (NO<sub>x</sub>) on a global scale (23% in  
49 2017, McDuffie et al., 2020) and across Europe (39% in 2017, EEA, 2019). In traffic environments, NO<sub>x</sub>  
50 consists mainly of nitric oxide (NO) and nitrogen dioxide (NO<sub>2</sub>), with the latter associated with a series  
51 of deleterious health effects (Nathan and Cunningham-Bussel, 2013; Brown, 2015; Atkinson et al., 2018).  
52 Moreover, NO<sub>x</sub> affects human health indirectly –through the production of surface ozone (O<sub>3</sub>) (Monks  
53 et al., 2015) and secondary inorganic aerosol (Fuzzi et al., 2015)– and impacts the environment –through  
54 eutrophication and acidification of sensitive ecosystems (Peel et al., 2013).

55 European countries, in particular those in the northwest, have pioneered strategies to tackle  
56 environmental issues, with prominent roles in the international community (Lieberink et al., 2009;  
57 Grennfelt et al., 2020). In that context, air pollution has been a major political concern in Europe since  
58 the late 1970s, leading to the development of ambient air quality standards and control of the major  
59 emissions sources (Crippa et al., 2016). In the case of road transport, new vehicles have had to meet  
60 increasingly stringent emission limits since the early 1990s, established by the so-called ‘Euro emission  
61 standards’ (European Commission, 2021). These standards are based on emission factors (EF) measured  
62 in laboratories under controlled conditions following regulatory driving cycles.

63 However, field studies revealed that the EF simulated with traffic emission models (COMputer  
64 Programme to calculate Emissions from Road Transport COPERT, and Handbook Emission Factors for  
65 Road Transport HBEFA), and validated with laboratory-based EF, largely underestimated the real  
66 exhaust emissions (Carslaw et al., 2011; Carslaw and Rhys-Tyler, 2013; Krecl et al., 2017). Because  
67 laboratory-based EF are used to compile the official national inventories for the road transport sector, it  
68 is of utmost importance to conduct real-world EF measurements to identify mismatches in the emission  
69 models (Franco et al., 2013). In light of this, the European Union through the Real Driving Emissions

70 mandates that laboratory tests be complemented with real driving condition tests for new passenger cars  
71 (PC) and light-commercial vehicles (LCV) since September 2019 (European Commission, 2021). On the  
72 other hand, to assess how EF has responded to policies on emission reduction and its long-term trend,  
73 we need to consider approaches based on continuous measurements over a long period. In that context,  
74 extended datasets of ambient air pollutant concentrations at roadside sites available in several European  
75 cities can be used.

76 In the case of nitrogen species, only NO<sub>x</sub> emissions are regulated for on-road vehicles in Europe, despite  
77 NO<sub>2</sub> being also directly emitted by vehicle exhausts (Carslaw et al., 2011). The NO<sub>2</sub>:NO<sub>x</sub> emission ratios  
78 largely increased in Europe in the period 1995-2010 (Grange et al., 2017), and the annual air quality  
79 standard for NO<sub>2</sub> was still exceeded at 10% of the European stations (329 out of 3260), mainly near roads  
80 (European Environmental Agency, 2019). This is particularly worrying since roadside stations are  
81 located in densely populated areas where population exposure can be large.

82 Based on unique long-term datasets, this study analyzed the trends of NO<sub>2</sub> and NO<sub>x</sub> concentrations at  
83 three curbside sites in three European cities: Copenhagen, London and Stockholm. Then, EF<sub>NO<sub>x</sub></sub> for the  
84 vehicle fleet were determined based on the street increment of the NO<sub>x</sub> concentrations and inverse  
85 modeling techniques. The NO<sub>2</sub>:NO<sub>x</sub> vehicles emission ratios were estimated using their respective  
86 ambient concentrations as proxies. We compare our EF<sub>NO<sub>x</sub></sub> values for the mixed fleet with EF extracted  
87 from databases and remote sensing studies. Finally, the temporal evolutions of EF<sub>NO<sub>x</sub></sub> and primary NO<sub>2</sub>  
88 emissions are discussed in relation to regional and local policies applied to mitigate the road transport  
89 emissions.

90

91

92

## 93 **2. Methods**

### 94 **2.1 Sampling sites and instrumentation**

95 We selected paired street canyon and urban background sites in Copenhagen, London and Stockholm,  
96 where long-term hourly NO<sub>x</sub> (NO+NO<sub>2</sub>), O<sub>3</sub> and traffic measurements were available. Another criterion  
97 was the availability of meteorological data at stations representative of winds above the corresponding  
98 street canyons (Table 1, and Supplementary Material). NO<sub>x</sub> and O<sub>3</sub> concentrations were measured using  
99 chemiluminescence and ultraviolet photometry analyzers, respectively, complying with European  
100 reference methods (EN14211, 2012; EN14625, 2012). Note that the measurements conducted at the air  
101 pollution and meteorological sites are subject to rigorous quality assurance procedures since they belong  
102 to national networks.

103 Hourly traffic data consisted of traffic volume (TR) and vehicle speed (VS). Traffic measurements were  
104 continuously recorded on Hornsgatan St. (Stockholm) (Krecl et al., 2017) and Marylebone Road  
105 (London) (Harrison et al., 2011) by using loop-profilers embedded in the surface. In the case of Jagtvej  
106 St. (Copenhagen), pre-defined traffic data profiles provided by the Danish Operational Street Pollution  
107 model (OSPM) were scaled up by the annual average daily traffic (AADT) and mean vehicle speed as  
108 described in the Supplementary Material, together with details of traffic data validation.

109

### 110 **2.2 Data processing**

#### 111 **2.2.1 Trend analysis of atmospheric concentrations**

112 Trends in air pollutant concentrations can be driven by changes in meteorological conditions, emissions,  
113 atmospheric chemistry or the built environment (Grange and Carslaw, 2019; Malley et al., 2018). When  
114 trend analysis is conducted for assessing the success of certain air quality management strategies, the  
115 influence of the weather conditions on ambient concentrations should be removed. Thus, we applied the

116 *rmweather* R package (version 0.1.51; Grange and Carslaw, 2019) on hourly concentrations measured at  
117 all sites to remove this influence. The package builds Random Forest models that predict hourly NO<sub>x</sub> (or  
118 NO<sub>2</sub>) concentrations based on several independent variables, and then estimates the meteorologically  
119 normalized series. We used the following explanatory variables: Unix date (number of seconds elapsed  
120 since Jan. 1, 1970) representing the trend term, Julian day (day of the year) as the seasonal trend, day of  
121 the week, hour of the day, and meteorological variables (Table 1). The importance of the predictor  
122 variables on the air pollutant concentrations was also assessed with the *rmweather* package. Further  
123 details on the model development and normalization technique are given in the Supplementary Material.  
124 The normalized hourly ambient concentrations were aggregated to mean monthly values, which were  
125 subsequently used to estimate linear trends by the non-parametric Theil-Sen method (Snell et al., 1996)  
126 for each pollutant and site over the common period (1998-2017). The Theil-Sen trend is a median slope  
127 trend line resistant to outliers. It was calculated with the *TheilSen* function available in the *openair* R  
128 package (Carslaw and Ropkins, 2012), which also computed the confidence intervals at 95% and *p*-  
129 values by bootstrap resampling.

130

### 131 **2.2.2 Calculation of NO<sub>2</sub>:NO<sub>x</sub> emission ratios**

132 We estimated the NO<sub>2</sub>:NO<sub>x</sub> vehicle emission ratios by filtering ambient concentrations of NO<sub>2</sub> and NO<sub>x</sub>  
133 measured at curbside sites following Grange et al. (2017). This technique isolates the primary NO<sub>2</sub>  
134 component by selecting measurements conducted in periods when the production of NO<sub>2</sub> via the NO+O<sub>3</sub>  
135 reaction is negligible. Thus, we chose only NO<sub>2</sub> and NO<sub>x</sub> concentrations corresponding to traffic-  
136 dominated periods (06:00-18:00 on weekdays), with low O<sub>3</sub> background concentrations. An O<sub>3</sub> threshold  
137 of 10 µg m<sup>-3</sup> was found appropriate to minimize the NO<sub>2</sub> secondary production and still have enough  
138 measurements for the emission ratio calculation (more details are provided in the Supplementary  
139 Material). For each curbside site and year combination, we calculated the slope of the robust linear

140 regression between the filtered NO<sub>x</sub> and NO<sub>2</sub> atmospheric concentrations, which is a proxy of the  
141 primary NO<sub>2</sub>:NO<sub>x</sub> emission ratio.

142

### 143 **2.2.3 Determination of EF<sub>NO<sub>x</sub></sub>**

144 For each street canyon and year, hourly EF<sub>NO<sub>x</sub></sub> [g veh<sup>-1</sup> m<sup>-1</sup>] were determined for the mixed fleet as  
145 follows (Ketzel et al., 2003; Krecl et al., 2018):

146

$$147 \quad EF_{NO_x} = \frac{\Delta NO_x(t) D(t)}{TR(t)}, \quad (1)$$

148

149 where ΔNO<sub>x</sub> [g m<sup>-3</sup>] is the measured increment concentration (curbside minus urban background  
150 concentrations) due to the emissions of vehicles driving on that street, TR [veh s<sup>-1</sup>] is the total traffic  
151 volume on that street, *D* [m<sup>2</sup> s<sup>-1</sup>] is the dilution rate and *t* is the time [s]. The dilution rate depends on  
152 wind conditions, traffic characteristics (TR and VS) and street canyon geometry, and was computed by  
153 inverse dispersion modeling using the OSPM (Berkowicz, 2000). Details on the inverse modeling  
154 technique can be found elsewhere (Palmgren et al., 1999; Ketzel et al., 2003).

155 The OSPM has been extensively tested (Kakosimos et al., 2010) and successfully simulates the NO<sub>x</sub>  
156 concentrations at regular street canyons, such as Jagtvej and Hornsgatan (Ottosen et al., 2015). However,  
157 an initial screening of our OSPM results revealed abnormally high *D* values (> 24 m<sup>2</sup> s<sup>-1</sup>) at Marylebone  
158 Road site associated with northerly winds with WS > 2.0 m s<sup>-1</sup>, which we attributed to the more complex  
159 street canyon geometry. This wind condition was not very frequent (12%), but may lead to the  
160 overestimation of both the dilution and the mean EF<sub>NO<sub>x</sub></sub> values if it prevails for certain hours. Thus, these  
161 occurrences were excluded from further analysis.



162 Only hourly  $EF_{NO_x}$  values for the period 07:00-23:00 on weekdays were considered for the analysis  
163 because (i) the fleet composition is rather similar between weekdays, and (ii) it avoids the large  
164 uncertainties in  $EF_{NO_x}$  calculations associated with the small street increments and low TR, typically  
165 observed in the early hours on weekdays (Krecl et al., 2018). Then, mean annual values were calculated  
166 for the years displayed in Table 1. Further details on  $EF_{NO_x}$  calculations and OSPM model setup are given  
167 in the Supplementary Material.

168

#### 169 **2.2.4 Validation with other databases**

170 The  $EF_{NO_x}$  computed by inverse modeling (Eq. 1) was compared with  $EF_{NO_x_w}$  calculated by aggregating  
171  $EF_{NO_x_{i,j,k}}$  per vehicle category and weighted according to each category share  $n$  within the fleet, as  
172 follows:

$$173 \quad EF_{NO_x_w} = \sum_{i,j,k} EF_{NO_x_{i,j,k}} \cdot n_{i,j,k}, \quad (2)$$

174

175 where the category is a combination of vehicle class  $i$ , fuel  $j$  and Euro standard stage  $k$ .

176  $EF_{NO_x_{i,j,k}}$  were extracted from three sources: (i) the European Monitoring and Evaluation Program  
177 (EMEP) guidebook (EMEP/EEA, 2019), (ii) HBEFA V.3.3 handbook processed for typical site-specific  
178 traffic conditions by Burman et al. (2019), and (iii) remote sensing studies conducted under urban driving  
179 conditions in Europe (UK: Carslaw et al., 2011; Carslaw and Rhys-Tyler, 2013; Carslaw et al., 2019;  
180 Ghaffarpasand et al., 2020, and Sweden: Liu et al., 2019; Zhou et al., 2020) (Table 2). We used the  
181 HBEFA  $EF_{NO_x}$  for ethanol and biogas since the other two sources do not include these fuels.

182 Individual  $EF_{NO_x}$  largely depends on the vehicle category, and the vehicle category share at national and  
183 municipal levels can largely differ from the typical share of the actual fleet driving on the canyon street

184 for the same year (Burman et al., 2019). Thus, we profited from the detailed in situ surveys of the vehicle  
185 fleet on Hornsgatan St. for the years 2009 and 2017 to validate our  $EF_{NOx}$  against the EMEP, HBEFA  
186 and remote sensing estimates. These surveys analyzed automatic number plate recordings of four million  
187 vehicles, and subsequent inquiry of vehicle information from the city municipality provided detailed  
188 composition of the fleet in terms of vehicle class, fuel and Euro standard stage (Burman et al., 2019).

189

### 190 **3. Results and Discussion**

#### 191 **3.1 Trends in ambient concentrations**

192 The most polluted street canyon was Marylebone Road (mean of  $NO_x$  and  $NO_2$  in 2017: 286.3 and 83.9  
193  $\mu g m^{-3}$ ), followed by Hornsgatan (79.9 and 35.3  $\mu g m^{-3}$ ) and Jagtvej (55.2 and 27.5  $\mu g m^{-3}$ ). The urban  
194 background air was cleanest in Stockholm (mean of  $NO_x$  and  $NO_2$  in 2017: 13.3 and 10.7  $\mu g m^{-3}$ )  
195 followed by Copenhagen (18.4 and 15.3  $\mu g m^{-3}$ ) and London (50.4 and 32.3  $\mu g m^{-3}$ ).

196 Figure 1 shows the monthly mean  $NO_x$  and  $NO_2$  concentrations measured at the street canyon and urban  
197 background sites in Copenhagen (1994-2017), London (1998-2017) and Stockholm (1992-2017),  
198 together with the street increments of  $NO_x$  and  $NO_2$  ( $\Delta NO_x$  and  $\Delta NO_2$ , respectively) and the normalized  
199 concentrations. Note that the mean  $NO_2$  annual limit of the EU air quality directive (40  $\mu g m^{-3}$ ) was  
200 exceeded every year at the street canyon sites in Copenhagen (1994-2009), London (1998-2017) and  
201 Stockholm (1992-2016), and the urban background site in London (1998-2003). The meteorologically  
202 normalized series show a decreasing trend in  $NO_x$ ,  $\Delta NO_x$  and (to a lesser extent)  $NO_2$  in Stockholm and  
203 Copenhagen over the years, but London presented either modest improvements or increase in  
204 concentrations at Marylebone Road (Figs. 1a-f). Over the period 1998-2017, Copenhagen and Stockholm  
205 showed similar patterns in concentration reductions: (i)  $NO_x$  decreased more at curbside (55-60%) than  
206 at urban background sites (41-52%), and (ii)  $NO_2$  reductions were smaller than  $NO_x$ , and declined more  
207 at urban background (35-46%) than at street canyon sites (27-35%). London exhibited a different

208 behavior, with the largest NO<sub>x</sub> reduction recorded at the urban background site (36%), and no reductions  
209 in NO<sub>2</sub> concentrations at the curbside site (Figs. 1b,e).

210 Although road transport dominates the total NO<sub>x</sub> emissions in Europe (EEA, 2019), other local and non-  
211 local sources might have contributed to ambient NO<sub>x</sub> concentrations at specific sites. Hence, by  
212 calculating the NO<sub>x</sub> increment at the street canyon sites the non-local contributions are filtered out,  
213 leaving only the traffic-related contributions from vehicles driving on that street. Street increments for  
214 NO<sub>2</sub> and NO<sub>x</sub> were higher for London compared to Stockholm and Copenhagen (Figs. 1g-i), which is  
215 consistent with the ADDT values recorded at the canyon streets in the period 1998-2017: 78300, 27500  
216 and 18900 respectively.

217 In general, the monthly mean concentrations at all sites showed a sawtooth pattern due to  
218 meteorologically driven effects on atmospheric mixing and transport and temperature-driven effects on  
219 emissions, which were removed after normalization (Fig. 1, orange lines). The analysis of the importance  
220 of the explanatory variables of the Random Forest models revealed that the nitrogen oxide concentrations  
221 within the street canyons were largely influenced by rooftop-level wind (WD and WS, Fig. S2a,  
222 Supplementary Material). This result agrees with Krecl et al. (2015), who reported that recirculation  
223 patterns governed the air pollution concentrations within Hornsgatan street canyon (Fig. S2a,  
224 Supplementary Material). For example, the site-dependent Random Forest model run in our study was  
225 able to capture the recirculation pattern at that site. The meteorologically normalized concentrations  
226 showed non-linear associations with WS, with dilution increasing with WS (e.g., Fig. S2b,d,  
227 Supplementary Material). The main predictor for the urban background sites was WS, with high NO<sub>x</sub>  
228 concentrations associated with low WS, as also reported by Krecl et al. (2011), while WD had negligible  
229 influence. This confirms that the sites can be taken as representative of urban background environment.  
230 Kamińska (2019) and Laña et al. (2016) found similar results at other European sites.

231 In general, seasonal trends played a modest role on NO<sub>x</sub> concentrations, with lower NO<sub>x</sub> values observed  
232 in summertime. This is most likely due to improved dispersion and reduced emissions, since summer  
233 presents lower traffic volume (long holidays) and higher ambient temperatures might decrease NO<sub>x</sub>  
234 emissions for the diesel fleet (Grange et al., 2019).

235 The trend analysis is very sensitive to the chosen period, as reported by several studies (Grange and  
236 Carslaw, 2019; Olstrup et al., 2018). Hence, we focused on the overlapping period 1998-2017 to avoid  
237 the influence of site-specific conditions outside these years. Overall, there was a significant downward  
238 trend in concentrations (Fig. 2), with NO<sub>x</sub> decreasing faster than NO<sub>2</sub> in the three cities. At the curbside  
239 sites, this pattern is explained by the higher NO<sub>2</sub>:NO<sub>x</sub> emission ratios due to the introduction of some  
240 exhaust treatments for diesel vehicles (that convert NO to NO<sub>2</sub>) and the accelerated penetration of diesel  
241 PC (Grange et al., 2017). At urban background sites, the NO<sub>2</sub> concentrations are mainly controlled by  
242 the photochemical conversion of locally emitted NO to NO<sub>2</sub> rather than direct NO<sub>2</sub> emissions (Keuken  
243 et al., 2009; Anttila and Tuovinen, 2010). In urban atmospheres highly impacted by NO<sub>x</sub> emissions, a  
244 reduction in NO concentrations reduces the consumption of O<sub>3</sub> by titration (Monks et al., 2015) and,  
245 specifically for Europe, the regional background O<sub>3</sub> has been increasing (0.20–0.59 μg m<sup>-3</sup> yr<sup>-1</sup> for the  
246 annual mean in 1995-2014, Yan et al., 2018). As a consequence, more O<sub>3</sub> is available to oxidize NO to  
247 NO<sub>2</sub>, causing a steeper downward trend of NO concentrations than NO<sub>2</sub> at the urban background sites.

248 To facilitate the comparison of the concentration trends among sites with different pollution levels,  
249 changes were also expressed as percentage of variation per year over the period 1998-2017 (Fig. 2). The  
250 reductions in NO<sub>x</sub> concentrations in the urban background atmosphere were comparable in Copenhagen  
251 and Stockholm (-2.1 and -2.6 % yr<sup>-1</sup>, respectively). In Denmark, the reduction in NO<sub>x</sub> emissions is due  
252 to the increasing use of catalysts in vehicles, and installation of low-NO<sub>x</sub> burners and denitrifying units  
253 in power plants and district heating plants (Nielsen et al., 2019). In Sweden, the total decline in NO<sub>x</sub>  
254 emissions is linked to more stringent road transport emission standards, increased use of district heating

255 and introduction of a NO<sub>x</sub> fee in 1992 for reducing industrial emissions (Swedish Environmental  
256 Protection Agency, 2020). Particularly, the former might be more relevant for Stockholm where road  
257 traffic is the dominant NO<sub>x</sub> source (Johansson et al., 2008). Note that changes in the urban atmosphere  
258 can be also affected by variations in the regional concentrations since they have non-negligible  
259 contributions (Ellermann et al., 2017; Krecl et al., 2011). The reduction in NO<sub>x</sub> concentrations in the  
260 urban background atmosphere of London was modest (-1.3 % yr<sup>-1</sup>) compared to the other two cities.

261 Figure 2 also shows that the negative trends of the NO<sub>x</sub> street increments in Copenhagen and Stockholm  
262 were even larger (-2.6 and -3.0 % yr<sup>-1</sup>, respectively) than at the urban background sites. These large drops  
263 were attributed to variations in the traffic emissions over time, since neither the street canyons nor the  
264 adjacent areas underwent any changes in their configuration, and concentrations were already  
265 meteorologically normalized. In Denmark, the largest source of NO<sub>x</sub> emissions is road transport (30%  
266 in 2017), with a 65% decrease in the period 1998-2017 (mean of -3.2 % yr<sup>-1</sup>) (Nielsen et al., 2019). Based  
267 on the emission inventories for Sweden in 1998 and 2017 (SCB, 2021), road traffic emissions were the  
268 main NO<sub>x</sub> sources and decreased 48.5% over the 20-year period, which corresponds to -2.4 % yr<sup>-1</sup>. Thus,  
269 this national reduction in traffic emissions is in the same order of the reduction in concentrations found  
270 at the street canyon (-3.0% yr<sup>-1</sup>). In the case of London, the main emission source for NO<sub>x</sub> was road  
271 transport (49%) in the year 2016 (Transport for London, 2016). Road transport also dominates the NO<sub>x</sub>  
272 emissions at national level in the UK (33% in 2017), with a reduction of 67% in the period 1998-2017  
273 (DEFRA, 2020). This represents a reduction of -3.3 % yr<sup>-1</sup> at UK level, which is far from the small street  
274 increment trend at Marylebone Road site (-0.2 % yr<sup>-1</sup>). This large discrepancy could be explained by the  
275 use of emission inventories built with EF<sub>NO<sub>x</sub></sub> that largely underestimate the real emissions in the UK  
276 (Carslaw et al., 2011; Carslaw and Rhys-Tyler, 2013) and/or changes in the vehicle fleet composition for  
277 certain streets.

278 In relation to the NO<sub>2</sub> concentration trends, both urban background and curbside sites showed long-term  
279 improvements, but smaller for the latter where traffic emissions dominate. London presented the smallest  
280 decreases in concentration, with slight positive NO<sub>2</sub> street increment but not statistically significant for  
281 the study period (1998-2017). The discussion on the NO<sub>2</sub>:NO<sub>x</sub> emission ratios is further developed in  
282 Section 3.2.

283

### 284 **3.2 Trends in EF for the vehicle fleet**

285 The annual evolutions of the EF<sub>NO<sub>x</sub></sub> for the vehicle fleet at the three curbside sites over the study period  
286 are displayed in Figs. 3a-c. The grey shadows represent the 95% confidence interval of the mean,  
287 calculated using the monthly mean values for each year and site. In general, the decreasing trends  
288 observed at Jagtvej and Hornsgatan sites for the mixed fleet (Fig. 3 a,c) match the temporal reduction in  
289 EF<sub>NO<sub>x</sub></sub> for different vehicle categories/fuel, as reported by remote sensing studies conducted in European  
290 urban areas (Tables 2). These results agree with the introduction of new technologies in the vehicle fleet  
291 to reduce air pollution emissions. However, the EF<sub>NO<sub>x</sub></sub> pattern was rather constant at Marylebone Road  
292 over the period (Fig. 3b), and showed a larger monthly variability.

293 Inspecting the normalized  $\Delta$ NO<sub>x</sub> trends (Figs. 3d-f), we can observe a clear resemblance between the  
294 EF<sub>NO<sub>x</sub></sub> trends for Copenhagen and Stockholm (Figs. 3a, c). However, note that the EF<sub>NO<sub>x</sub></sub> value was  
295 reported as the mean of the mixed fleet per vehicle whereas the normalized  $\Delta$ NO<sub>x</sub> does not consider  
296 variations in traffic patterns (volume, speed, or vehicle type share). For example, the “bump” observed  
297 in the EF<sub>NO<sub>x</sub></sub> time series at Hornsgatan site in the period 2011-2017 (Fig. 3c) coincided with the reduction  
298 in the total TR observed since January 2010, when a ban on studded tires was introduced for the  
299 wintertime and which remained over the years (Norman et al., 2016). The normalized  $\Delta$ NO<sub>x</sub> was flat for  
300 the same period (Fig. 3f), suggesting that total NO<sub>x</sub> emissions might have not changed, but increased per  
301 vehicle. We hypothesize that this increase in EF<sub>NO<sub>x</sub></sub> for the mixed fleet at Hornsgatan site could have

302 been caused by the introduction of buses fueled with 100% Rapeseed Methyl Ester (RME) in 2011, as  
303 part of the city of Stockholm's strategy for running the entire bus fleet on renewable fuels and to comply  
304 with the Clean Vehicles Directive (2009/33/EC). Note that RME buses emit on average 2.5 times more  
305 NO<sub>x</sub> than the diesel ones with similar engine and after-treatment technology (Table S2, E5 and Selective  
306 Catalytic Reduction SCR). In the year 2011, 10% of the public bus fleet was fueled with 100% RME  
307 (Johan Böhlin, personal communication, Feb. 2021), and the RME bus consumption doubled in 2014  
308 (Clean Fleets, 2014). This information is consistent with the fast increase in RME sales in the Stockholm  
309 county in the period 2011-2017 (Stockholms stad, 2021). The reduction observed in EF<sub>NO<sub>x</sub></sub> after the year  
310 2015 might be mainly associated with the introduction of newer bus engines and/or cleaner exhaust after-  
311 treatment technologies for NO<sub>x</sub> emissions.

312 The  $\Delta$ NO<sub>x</sub> trend at Marylebone Road demonstrates that, despite all the measures implemented for NO<sub>x</sub>  
313 control, the total emission remained stable since 2002. According to Font and Fuller (2016), the  $\Delta$ NO<sub>x</sub>  
314 trends in London showed a large spatial heterogeneity in the period 2005-2014. They found that  
315 increasing  $\Delta$ NO<sub>x</sub> trends were experienced on streets with increasing number of buses per day, such as  
316 Marylebone Road in 2010-2014. Conversely,  $\Delta$ NO<sub>x</sub> reductions were associated with a lower traffic  
317 volume of buses and/or retrofitted buses with cleaner technologies (such as SCR + Diesel Particulate  
318 Filter DPF, Carslaw et al., 2015).

319 The time evolution of the NO<sub>2</sub>:NO<sub>x</sub> emission ratios for the vehicle fleet is displayed in Figs. 3g-i for the  
320 three canyon sites. The interpretation is complex because the mean emission ratio for the whole fleet is  
321 influenced by the large variation observed with vehicle category/fuel and Euro standard stage (Tables 2).  
322 The fraction of primary NO<sub>2</sub> emissions also depends on the exhaust after-treatment (particularly for  
323 buses, Table S2, Supplementary Material), vehicle mileage (Carslaw et al., 2019), mean VS (Grice et al.,  
324 2009), ambient temperature (Grange et al., 2019), and engine load (Carslaw et al., 2011; Carslaw and  
325 Rhys-Tyler, 2013). Moreover, differences in emission ratios vary considerably from manufacturer to

326 manufacturer even for the same Euro standard stage and model year (Bernard et al., 2018; Carslaw et al.,  
327 2019).

328 Grange et al. (2017) showed a clear positive trend in annual mean NO<sub>2</sub>:NO<sub>x</sub> emission ratios for 61  
329 European cities between 1995 and 2010. This trend can be attributed to the wide use of diesel oxidation  
330 catalysts (DOC) on PC –that target CO and hydrocarbons, but intentionally convert NO into NO<sub>2</sub> (Fiebig  
331 et al., 2014; Russell and Epling, 2011). Remote sensing studies confirm the increase of the NO<sub>2</sub>:NO<sub>x</sub>  
332 emission ratios with the introduction of DOC in E3 diesel PC (Table 2). The overall impact of these  
333 primary NO<sub>2</sub> emissions became important due to the dieselization of the European PC fleet, driven by  
334 improvements in fuel economy and supposed CO<sub>2</sub> emission reduction (Cames and Helmers, 2013).

335 This dieselization process was strong in the three countries (Figs. 3j-1) with the help of government  
336 incentives (Cames and Helmers, 2013). Even though the emission ratios are slightly higher for diesel  
337 LCV than for diesel PC for certain Euro stages (Table 2), diesel PC have become abundant at national  
338 and urban street levels in more recent times. For example, the shares of diesel PC and LCV in relation to  
339 the total fleet on Hornsgatan St. were 33 and 13% in 2017 vs. 17 and 11% in 2009. Note that when the  
340 shift towards the use of diesel fuel in PC at the expense of gasoline occurred, increasing NO<sub>2</sub>:NO<sub>x</sub>  
341 emission ratios were clearly observed at Jagtvej and Hornsgatan sites until 2008 and 2010, respectively  
342 (Figs. 3g,i). The decay in primary NO<sub>2</sub> emissions observed afterwards might be explained by the  
343 development of more efficient DOC systems by the car manufacturers (Carslaw et al., 2016; Carslaw et  
344 al., 2019). E6 standards introduced tighter limits for NO<sub>x</sub> emissions, and diesel PC were also equipped  
345 with NO<sub>x</sub> after-treatment systems that increased the NO<sub>2</sub>:NO<sub>x</sub> emission ratios again (Table 2, E6).

346 Jagtvej and Hornsgatan experienced this increase in emission ratios but differences in time and magnitude  
347 might be explained by the composition of the diesel PC fleet per manufacturer group, given the large  
348 variations reported by Carslaw et al. (2019). Finally, the absolute NO<sub>x</sub> and NO<sub>2</sub> emissions remained low



349 in the period matching the E6 stage, and reductions in  $\Delta\text{NO}_x$  and  $\Delta\text{NO}_2$  were found at Jagtvej (Figs. 2g,j)  
350 and Hornsgatan sites (Figs. 2i,l).

351 Note that certain particular characteristics of the vehicle fleet might arise when analyzing the behavior  
352 of  $\text{NO}_2:\text{NO}_x$  emission ratios for individual cities and sites. Notably, Marylebone Road showed the  
353 maximum peak value (23 vol. %) in 2005 and dropped thereafter (Fig. 3h). This site was largely affected  
354 by changes in the urban bus engines and exhaust after-treatment technologies, since the number of buses  
355 operating on that street is high (e.g., 1473 buses per weekday in 2003). For example, the steep increase  
356 in ratios observed between 2002 and 2003 was attributed to the retrofitting program of London urban  
357 buses (E3 stage) with continuously regenerating particle traps (formed by a combination of DOC and  
358 DPF, Grange and Carslaw, 2019) and an increase in buses as part of the London congestion charge  
359 scheme (Givoni, 2012). The decline in ratios after 2008 was linked to the introduction of buses with  
360 newer and cleaner technologies and removal of old buses (Grange and Carslaw, 2019). The peak and  
361 decay of  $\text{NO}_2:\text{NO}_x$  at Marylebone Road were observed earlier than those in inner London (Carslaw et  
362 al., 2016) and we hypothesize that this shift might be due to the different implementation stages in the  
363 bus retrofitting programs and bus fleet renewal, depending on the analyzed street. Even though buses  
364 largely influence the emissions at Marylebone Road, the contribution of the diesel PC to the emission  
365 ratios cannot be ruled out because of their large number (Fig. 3k).

366

### 367 **3.3 Comparison of $\text{EF}_{\text{NO}_x}$ at Hornsgatan with literature data**

368 Figure 4 shows the mean  $\text{EF}_{\text{NO}_x}$  for the mixed fleet at Hornsgatan site in the years 2009 and 2017  
369 extracted from the EMEP and HBEFA databases, urban remote sensing studies (Table 2), and the results  
370 based on inverse modeling. Regardless of the method, lower  $\text{EF}_{\text{NO}_x}$  values were found in 2017 than in  
371 2009, following the general trend of decreasing  $\text{NO}_x$  emissions with the introduction of new engines and  
372 after-treatment systems.

373 For both years, the EMEP-based  $EF_{NO_x}$  presented the lowest values (0.73 and 0.51  $g\ km^{-1}\ veh^{-1}$  in 2009  
374 and 2017, respectively), whereas the results based on HBEFA and remote sensing studies were very  
375 similar (1.13 and 1.19  $g\ km^{-1}\ veh^{-1}$  in 2009; 0.92 and 0.98  $g\ km^{-1}\ veh^{-1}$  in 2017). This similarity might be  
376 explained by the update of the HBEFA database (V.3.3) with  $EF_{NO_x}$  of diesel PC for E4-E6 stages,  
377 considering new laboratory and real-world measurements (portable emission monitoring systems and  
378 remote sensing data), after compelling evidence that these EF were lower than in-use vehicles studies  
379 (Carslaw et al., 2011; Carslaw and Rhys-Tyler, 2013). The  $EF_{NO_x}$  presented in the EMEP guidebook  
380 were developed with the COPERT model, which has been reported to predict lower NO<sub>x</sub> emissions than  
381 the HBEFA database under stop-and-go traffic conditions in cities, particularly for diesel vehicles (Borge  
382 et al., 2012). A recent UK study (Davison et al., 2021) also found that the national inventory –that heavily  
383 relies on the COPERT database– underestimates the NO<sub>x</sub> emissions from PC and LCV up to 47% in  
384 urban areas compared with emissions calculated with real-world  $EF_{NO_x}$  from remote sensing studies.  
385 The inverse modeling results presented the highest mean values for both years (1.72 and 1.35  $g\ km^{-1}\ veh^{-1}$   
386 <sup>1</sup> in 2009 and 2017, respectively). The weighted  $EF_{NO_x}$  calculations at Hornsgatan street using mean  
387 values per vehicle category from remote sensing data (Table 2) was a conservative approach. Considering  
388 the upper 95% confidence interval of  $EF_{NO_x}$  for each vehicle category yielded weighted  $EF_{NO_x}$  values  
389 much closer to those obtained with inverse modeling (1.69 and 1.23  $g\ km^{-1}\ veh^{-1}$  in 2009 and 2017,  
390 respectively). Moreover, most of the remote sensing studies were conducted in the UK (Table 2), where  
391 ambient conditions and the mix of on-road vehicle manufacturers and engine sizes might be different  
392 from Hornsgatan St. Thus, all these factors could have contributed to the  $EF_{NO_x}$  differences between  
393 inverse modeling and remote sensing methods.

394

### 395 **3.4 Study strengths and limitations**

396 As far as we know, this is the first study to analyze the trends of real-world  $EF_{NO_x}$  for the vehicle fleet at  
397 the same locations over two decades. Previous studies analyzed  $NO_x$  emission trends using only street  
398 increment concentrations as a proxy, or remote sensing measurements. Our approach (inverse modeling)  
399 presents advantageous features since: (i) we delivered  $EF_{NO_x}$  rather than  $NO_x$  street increments; this  
400 means that we addressed variations in traffic patterns that can largely influence emissions, and (ii) we  
401 assessed the overall effectiveness of policies for reducing the fleet emissions over a long time period.  
402 Although remote sensing studies provide individual  $EF_{NO_x}$  for a large vehicle sample, they might not  
403 cover the entire fleet particularly on busy roads with several lanes. Moreover, remote sensing field  
404 campaigns are short and traffic and ambient conditions might not be representative of the entire year.  
405 This study was limited to the analysis of three paired sites because of the reduced availability of long-  
406 term measurements. Hence the transferability of the results to other streets in the same cities should be  
407 done cautiously, considering site-specific features and local traffic policies.

408

#### 409 **4. Conclusions**

410 The Euro standard limits for new road vehicles have been successful in reducing  $NO_x$  vehicle emissions  
411 in the studied sites and the ambient concentrations over time, except for Marylebone Road. This busy  
412 street canyon –which experienced an increase in bus traffic since 2003– masked the modest effects of  
413 the Euro standard limits on citywide road traffic emissions in London, as shown by the reduction in  $NO_x$   
414 concentrations in the urban background atmosphere. The  $NO_2:NO_x$  emission ratios showed a positive  
415 trend until 2008-2010, which was also reflected in the  $NO_2$  ambient concentrations. This increase was  
416 associated with a strong dieselization process and the introduction of new after-treatment technologies  
417 that targeted the emission reduction of other species (greenhouse gases, carbon monoxide or particulate  
418 matter). Thus, while regulations on ambient concentrations of specific species have positive effects on  
419 human health, the overall outcomes should be considered before widely adopting them.

420 Our results suggest revising the low  $EF_{NOx}$  values presented in the EMEP guidebook for vehicle  
421 emissions, since they are used to compile official national inventories in Europe, estimate the exposures  
422 of population to air pollutants and of ecosystems to acidification and eutrophication. Finally, this work  
423 showed the relevance of long-term observations combined with dispersion modeling to detect trends, to  
424 assess the effectiveness of programs aimed at improving the urban air quality, and to validate emission  
425 estimates based on models and laboratory tests.

426

### 427 **Supplementary Material**

428 Details of air pollution sampling sites, traffic data, meteorological normalization of ambient  
429 concentrations, calculation of  $NO_2:NOx$  ratios, determination of  $EF_{NOx}$  for the mixed fleet, partial  
430 dependence plots, and review of real-world  $EF_{NOx}$  for urban buses are available.

431

### 432 **Acknowledgments**

433 We acknowledge Lars Burman (Stockholm Environment and Health Administration) and Johan Böhlin  
434 (Stockholm Public Transport, SL) for detailed data and comments on Stockholm traffic emissions. P.  
435 Krecl's work was funded by grant 305145/2020-7 from the National Council for Scientific and  
436 Technological Development of Brazil (CNPq).

437

### 438 **References**

439

- 440 Anttila, P., Tuovinen, J.P., 2010. Trends of primary and secondary pollutant concentrations in Finland  
441 in 1994-2007. *Atmos. Environ.* 44, 30–41. <https://doi.org/10.1016/j.atmosenv.2009.09.041>
- 442 Atkinson, R.W., Butland, B.K., Anderson, H.R., Maynard, R.L., 2018. Long-term concentrations of  
443 nitrogen dioxide and mortality, *Epidemiology*. <https://doi.org/10.1097/EDE.0000000000000847>
- 444 Berkowicz, R., 2000. OSPM: A Parameterised Street Pollution Model. *Environ. Monit. Assess.* 65,  
445 323–331.
- 446 Bernard, Y., Tietge, U., German, J., Muncrief, R., Foundation, F.I.A., Transportation, I.C. on C.,  
447 NCAP, G., Environment, T. and, Cities, C., 2018. Determination of Real-World Emissions from

448 Passenger Vehicles using Remote Sensing Data 31p.

449 Borge, R., de Miguel, I., de la Paz, D., Lumbreras, J., Pérez, J., Rodríguez, E., 2012. Comparison of  
450 road traffic emission models in Madrid (Spain). *Atmos. Environ.* 62, 461–471.  
451 <https://doi.org/10.1016/j.atmosenv.2012.08.073>

452 Brown, J.S., 2015. Nitrogen dioxide exposure and airway responsiveness in individuals with asthma.  
453 *Inhal. Toxicol.* 27, 1–14. <https://doi.org/10.3109/08958378.2014.979960>

454 Burman, L.; Elmgren, M.; Norman, M., 2019. Fordonsmätningar på Hornsgatan år 2017.

455 Cames, M., Helmers, E., 2013. Critical evaluation of the European diesel car boom - Global  
456 comparison, environmental effects and various national strategies. *Environ. Sci. Eur.* 25, 1–22.  
457 <https://doi.org/10.1186/2190-4715-25-15>

458 Carslaw, D.C., Beevers, S.D., Tate, J.E., Westmoreland, E.J., Williams, M.L., 2011. Recent evidence  
459 concerning higher NO<sub>x</sub> emissions from passenger cars and light duty vehicles. *Atmos. Environ.*  
460 45, 7053–7063. <https://doi.org/10.1016/j.atmosenv.2011.09.063>

461 Carslaw, D.C., Farren, N.J., Vaughan, A.R., Drysdale, W.S., Young, S., Lee, J.D., 2019. The  
462 diminishing importance of nitrogen dioxide emissions from road vehicle exhaust. *Atmos. Environ.*  
463 X 1, 100002. <https://doi.org/10.1016/j.aeaoa.2018.100002>

464 Carslaw, D.C., Murrells, T.P., Andersson, J., Keenan, M., 2016. Have vehicle emissions of primary  
465 NO<sub>2</sub> peaked? *Faraday Discuss.* 189, 439–454. <https://doi.org/10.1039/c5fd00162e>

466 Carslaw, D.C., Priestman, M., Williams, M.L., Stewart, G.B., Beevers, S.D., 2015. Performance of  
467 optimised SCR retrofit buses under urban driving and controlled conditions. *Atmos. Environ.* 105,  
468 70–77. <https://doi.org/10.1016/j.atmosenv.2015.01.044>

469 Carslaw, D.C., Rhys-Tyler, G., 2013. New insights from comprehensive on-road measurements of  
470 NO<sub>x</sub>, NO<sub>2</sub> and NH<sub>3</sub> from vehicle emission remote sensing in London, UK. *Atmos. Environ.* 81,  
471 339–347. <https://doi.org/10.1016/j.atmosenv.2013.09.026>

472 Carslaw, D.C., Ropkins, K., 2012. Openair - An R package for air quality data analysis. *Environ.*  
473 *Model. Softw.* 27–28, 52–61. <https://doi.org/10.1016/j.envsoft.2011.09.008>

474 Clean Fleets, 2014. Clean Buses – Experiences with Fuel and Technology Options 1–42.

475 Crippa, M., Janssens-Maenhout, G., Dentener, F., Guizzardi, D., Sindelarova, K., Muntean, M., Van  
476 Dingenen, R., Granier, C., 2016. Forty years of improvements in European air quality: Regional  
477 policy-industry interactions with global impacts. *Atmos. Chem. Phys.* 16, 3825–3841.  
478 <https://doi.org/10.5194/acp-16-3825-2016>

479 Davison, J., Rose, R.A., Farren, N.J., Wagner, R.L., Murrells, T.P., Carslaw, D.C., 2021. Verification  
480 of a National Emission Inventory and Influence of On-road Vehicle Manufacturer-Level  
481 Emissions. *Environ. Sci. Technol.* <https://doi.org/10.1021/acs.est.0c08363>

482 DEFRA. Statistical data set ENV01 - Emissions of air pollutants. Annual update to tables on emissions  
483 of important air pollutants in the UK [WWW Document], n.d. URL  
484 <https://www.gov.uk/government/statistical-data-sets/env01-emissions-of-air-pollutants> (accessed  
485 3.27.21).

486 EEA. European Union emission inventory report 1990-2017. EEA Report. No 08/2019, 2019.

487 Ellermann, T., Nygaard, J., Klenø Nøjgaard, J., Nordstrøm, C., Brandt, J., Christensen, J., Ketzel, M.,  
488 Massling, A., Bossi, R., Solvang Jensen, S., 2017. AU Scientific Report from DCE-Danish Centre  
489 for Environment and Energy THE DANISH AIR QUALITY MONITORING PROGRAMME  
490 Annual Summary for 2017.

491 EMEP/EEA, 2019. Air Pollutant Emission Inventory Guidebook 2019, EEA Report No 13/2019.  
492 EN14211. Ambient air — Standard method for the measurement of the concentration of nitrogen  
493 dioxide and nitrogen monoxide by chemiluminescence, 2012. . Brussels.

494 EN14625. Ambient air - Standard method for the measurement of the concentration of ozone by  
495 ultraviolet photometry. CEN. Brussels, 2012.

496 European Commission. Emissions in the automotive sector [WWW Document], 2021. URL  
497 [https://ec.europa.eu/growth/sectors/automotive/environment-protection/emissions\\_en](https://ec.europa.eu/growth/sectors/automotive/environment-protection/emissions_en) (accessed  
498 3.27.21).

499 European Environmental Agency, 2019. European Environmental Agency. Air quality in Europe —  
500 2019 report.

501 Fiebig, M., Wiartalla, A., Holderbaum, B., Kiesow, S., 2014. Particulate emissions from diesel engines:  
502 Correlation between engine technology and emissions. *J. Occup. Med. Toxicol.* 9, 1–18.  
503 <https://doi.org/10.1186/1745-6673-9-6>

504 Font, A., Fuller, G.W., 2016. Did policies to abate atmospheric emissions from traffic have a positive  
505 effect in London? *Environ. Pollut.* 218, 463–474. <https://doi.org/10.1016/j.envpol.2016.07.026>

506 Franco, V., Kousoulidou, M., Muntean, M., Ntziachristos, L., Hausberger, S., Dilara, P., 2013. Road  
507 vehicle emission factors development: A review. *Atmos. Environ.* 70, 84–97.  
508 <https://doi.org/10.1016/j.atmosenv.2013.01.006>

509 Fuzzi, S., Baltensperger, U., Carslaw, K., Decesari, S., Denier Van Der Gon, H., Facchini, M.C.,  
510 Fowler, D., Koren, I., Langford, B., Lohmann, U., Nemitz, E., Pandis, S., Riipinen, I., Rudich, Y.,  
511 Schaap, M., Slowik, J.G., Spracklen, D. V., Vignati, E., Wild, M., Williams, M., Gilardoni, S.,  
512 2015. Particulate matter, air quality and climate: Lessons learned and future needs. *Atmos. Chem.*  
513 *Phys.* 15, 8217–8299. <https://doi.org/10.5194/acp-15-8217-2015>

514 Ghaffarpasand, O., Beddows, D.C.S., Ropkins, K., Pope, F.D., 2020. Real-world assessment of vehicle  
515 air pollutant emissions subset by vehicle type, fuel and EURO class: New findings from the recent  
516 UK EDAR field campaigns, and implications for emissions restricted zones. *Sci. Total Environ.*  
517 734, 139416. <https://doi.org/10.1016/j.scitotenv.2020.139416>

518 Givoni, M., 2012. Re-assessing the results of the London congestion charging scheme. *Urban Stud.* 49,  
519 1089–1105. <https://doi.org/10.1177/0042098011417017>

520 Grange, S. K.; Farren, N. J.; Vaughan, A. R.; Rose, R. A.; Carslaw, D.C., 2019. Strong temperature  
521 dependence for light-duty diesel vehicle NO<sub>x</sub> emissions. *Environ. Sci. Technol.* 53, 6587–6596.

522 Grange, S.K., Carslaw, D.C., 2019. Using meteorological normalisation to detect interventions in air  
523 quality time series. *Sci. Total Environ.* 653, 578–588.  
524 <https://doi.org/10.1016/j.scitotenv.2018.10.344>

525 Grange, S.K., Lewis, A.C., Moller, S.J., Carslaw, D.C., 2017. Lower vehicular primary emissions of  
526 NO<sub>2</sub> in Europe than assumed in policy projections. *Nat. Geosci.* 10, 914–918.  
527 <https://doi.org/10.1038/s41561-017-0009-0>

528 Grennfelt, P., Engleryd, A., Forsius, M., Hov, Ø., Rodhe, H., Cowling, E., 2020. Acid rain and air  
529 pollution: 50 years of progress in environmental science and policy. *Ambio* 49, 849–864.  
530 <https://doi.org/10.1007/s13280-019-01244-4>

531 Grice, S., Stedman, J., Kent, A., Hobson, M., Norris, J., Abbott, J., Cooke, S., 2009. Recent trends and  
532 projections of primary NO<sub>2</sub> emissions in Europe. *Atmos. Environ.* 43, 2154–2167.  
533 <https://doi.org/10.1016/j.atmosenv.2009.01.019>

534 Harrison, R.M., Beddows, D.C.S., Dall’Osto, M., 2011. PMF analysis of wide-range particle size  
535 spectra collected on a major highway. *Environ. Sci. Technol.* 45, 5522–5528.  
536 <https://doi.org/10.1021/es201998m>

537 International Council on Clean Transportation, 2018. European vehicle market statistics, Pocketbook  
538 2018/19 63.

539 Johansson, C., Andersson, C., Bergström, R., Krecl, P., 2008. ITM-rapport 175.

540 Kakosimos, K.E., Hertel, O., Ketzler, M., Berkowicz, R., 2010. Operational Street Pollution Model  
541 (OSPM) - A review of performed application and validation studies, and future prospects.  
542 *Environ. Chem.* 7, 485–503. <https://doi.org/10.1071/EN10070>

543 Kamińska, J.A., 2019. A random forest partition model for predicting NO<sub>2</sub> concentrations from traffic

544 flow and meteorological conditions. *Sci. Total Environ.* 651, 475–483.  
545 <https://doi.org/10.1016/j.scitotenv.2018.09.196>

546 Ketzel, M., Wåhlin, P., Berkowicz, R., Palmgren, F., 2003. Particle and trace gas emission factors  
547 under urban driving conditions in Copenhagen based on street and roof-level observations. *Atmos.*  
548 *Environ.* 37, 2735–2749. [https://doi.org/10.1016/S1352-2310\(03\)00245-0](https://doi.org/10.1016/S1352-2310(03)00245-0)

549 Keuken, M., Roemer, M., van den Elshout, S., 2009. Trend analysis of urban NO<sub>2</sub> concentrations and  
550 the importance of direct NO<sub>2</sub> emissions versus ozone/NO<sub>x</sub> equilibrium. *Atmos. Environ.* 43,  
551 4780–4783. <https://doi.org/10.1016/j.atmosenv.2008.07.043>

552 Krecl, P., Johansson, C., Targino, A.C., Ström, J., Burman, L., 2017. Trends in black carbon and size-  
553 resolved particle number concentrations and vehicle emission factors under real-world conditions.  
554 *Atmos. Environ.* 165, 155–168. <https://doi.org/10.1016/j.atmosenv.2017.06.036>

555 Krecl, P., Targino, A.C., Johansson, C., 2011. Spatiotemporal distribution of light-absorbing carbon  
556 and its relationship to other atmospheric pollutants in Stockholm. *Atmos. Chem. Phys.* 11, 11553–  
557 11567. <https://doi.org/10.5194/acp-11-11553-2011>

558 Krecl, P., Targino, A.C., Johansson, C., Ström, J., 2015. Characterisation and source apportionment of  
559 submicron particle number size distributions in a busy street canyon. *Aerosol Air Qual. Res.* 15,  
560 220–233. <https://doi.org/10.4209/aaqr.2014.06.0108>

561 Krecl, P., Targino, A.C., Landi, T.P., Ketzel, M., 2018. Determination of black carbon, PM<sub>2.5</sub>, particle  
562 number and NO<sub>x</sub> emission factors from roadside measurements and their implications for  
563 emission inventory development. *Atmos. Environ.* 186, 229–240.  
564 <https://doi.org/10.1016/j.atmosenv.2018.05.042>

565 Laña, I., Del Ser, J., Padró, A., Vélez, M., Casanova-Mateo, C., 2016. The role of local urban traffic  
566 and meteorological conditions in air pollution: A data-based case study in Madrid, Spain. *Atmos.*  
567 *Environ.* 145, 424–438. <https://doi.org/10.1016/j.atmosenv.2016.09.052>

568 Liefferink, D., Arts, B., Kamstra, J., Ooijevaar, J., 2009. Leaders and laggards in environmental policy:  
569 A quantitative analysis of domestic policy outputs. *J. Eur. Public Policy* 16, 677–700.  
570 <https://doi.org/10.1080/13501760902983283>

571 Liu, Q., Hallquist, Å.M., Fallgren, H., Jerksjö, M., Jutterström, S., Salberg, H., Hallquist, M., Le  
572 Breton, M., Pei, X., Pathak, R.K., Liu, T., Lee, B., Chan, C.K., 2019. Roadside assessment of a  
573 modern city bus fleet: Gaseous and particle emissions. *Atmos. Environ.* X 3, 100044.  
574 <https://doi.org/10.1016/j.aeaoa.2019.100044>

575 Malley, C.S., Von Schneidemesser, E., Moller, S., Braban, C.F., Kevin Hicks, W., Heal, M.R., 2018.  
576 Analysis of the distributions of hourly NO<sub>2</sub> concentrations contributing to annual average NO<sub>2</sub>  
577 concentrations across the European monitoring network between 2000 and 2014. *Atmos. Chem.*  
578 *Phys.* 18, 3563–3587. <https://doi.org/10.5194/acp-18-3563-2018>

579 McDuffie, E.E., Smith, S.J., O'Rourke, P., Tibrewal, K., Venkataraman, C., Marais, E.A., Zheng, B.,  
580 Crippa, M., Brauer, M., Martin, R. V., 2020. A global anthropogenic emission inventory of  
581 atmospheric pollutants from sector- And fuel-specific sources (1970-2017): An application of the  
582 Community Emissions Data System (CEDs). *Earth Syst. Sci. Data* 12, 3413–3442.  
583 <https://doi.org/10.5194/essd-12-3413-2020>

584 Monks, P.S., Archibald, A.T., Colette, A., Cooper, O., Coyle, M., Derwent, R., Fowler, D., Granier, C.,  
585 Law, K.S., Mills, G.E., Stevenson, D.S., Tarasova, O., Thouret, V., Von Schneidemesser, E.,  
586 Sommariva, R., Wild, O., Williams, M.L., 2015. Tropospheric ozone and its precursors from the  
587 urban to the global scale from air quality to short-lived climate forcer. *Atmos. Chem. Phys.* 15,  
588 8889–8973. <https://doi.org/10.5194/acp-15-8889-2015>

589 Nathan, C., Cunningham-Bussel, A., 2013. Beyond oxidative stress: An immunologist's guide to  
590 reactive oxygen species. *Nat. Rev. Immunol.* 13, 349–361. <https://doi.org/10.1038/nri3423>

591 Nielsen, O. -K.; Plejdrup, M. S.; Winther, M.; Mikkelsen, M. H.; Nielsen, M.; Gyldenkerne, S.;

592 Fauser, P.; Albrektsen, R.; Hjelgaard, K. H.; Bruun, H. G.; Thomsen, M., 2019. Annual Danish  
593 Informative Inventory Report to UNECE. Emission inventories from the base year of the protocols  
594 to year 2017.

595 Norman, M., Sundvor, I., Denby, B.R., Johansson, C., Gustafsson, M., Blomqvist, G., Janhäll, S., 2016.  
596 Modelling road dust emission abatement measures using the NORTRIP model: Vehicle speed and  
597 studded tyre reduction. *Atmos. Environ.* 134, 96–108.  
598 <https://doi.org/10.1016/j.atmosenv.2016.03.035>

599 Olstrup, H., Forsberg, B., Orru, H., Nguyen, H., Molnár, P., Johansson, C., 2018. Trends in air  
600 pollutants and health impacts in three Swedish cities over the past three decades. *Atmos. Chem.*  
601 *Phys.* 18, 15705–15723. <https://doi.org/10.5194/acp-18-15705-2018>

602 Ottosen, T.B., Kakosimos, K.E., Johansson, C., Hertel, O., Brandt, J., Skov, H., Berkowicz, R.,  
603 Ellermann, T., Jensen, S.S., Ketzler, M., 2015. Analysis of the impact of inhomogeneous emissions  
604 in the Operational Street Pollution Model (OSPM). *Geosci. Model Dev.* 8, 3231–3245.  
605 <https://doi.org/10.5194/gmd-8-3231-2015>

606 Palmgren, F., Berkowicz, R., Ziv, A., Hertel, O., 1999. Actual car fleet emissions estimated from urban  
607 air quality measurements and street pollution models. *Sci. Total Environ.* 235, 101–109.  
608 [https://doi.org/10.1016/S0048-9697\(99\)00196-5](https://doi.org/10.1016/S0048-9697(99)00196-5)

609 Peel, J.L., Haeuber, R., Garcia, V., Russell, A.G., Neas, L., 2013. Impact of nitrogen and climate  
610 change interactions on ambient air pollution and human health. *Biogeochemistry* 114, 121–134.  
611 <https://doi.org/10.1007/s10533-012-9782-4>

612 Russell, A., Epling, W.S., 2011. Diesel oxidation catalysts. *Catal. Rev. - Sci. Eng.* 53, 337–423.  
613 <https://doi.org/10.1080/01614940.2011.596429>

614 SCB. Emissions of air pollutants from domestic transport by mode of transport. Year 1990 – 2019  
615 [WWW Document], 2021. URL  
616 [https://www.statistikdatabasen.scb.se/pxweb/en/ssd/START\\_\\_MI\\_\\_MI0108/MI0108InTransp/](https://www.statistikdatabasen.scb.se/pxweb/en/ssd/START__MI__MI0108/MI0108InTransp/)  
617 (accessed 3.27.21).

618 Snell, J., Birkes, D., Dodge, Y., 1996. *Alternative Methods of Regression*, Wiley Seri. ed, *Journal of*  
619 *the Royal Statistical Society. Series A (Statistics in Society)*. Wiley-Interscience.  
620 <https://doi.org/10.2307/2983483>

621 Stockholms stad. Proportion of environmental fuel in the Stockholm county [WWW Document], n.d.  
622 URL <http://miljobarometern.stockholm.se/miljomal/miljoprogram-2016-2019/miljoanpassade-transporter/minskat-fossilberoende/andel-miljobransle-i-stockholms-lan/rapsbransle/table/>  
623 (accessed 3.27.21).

624

625 Swedish Environmental Protection Agency, Informative Inventory Report Sweden 2020, 2020.

626 Transport for London. London Atmospheric Emissions Inventory (LAEI) 2016 [WWW Document],  
627 n.d. URL <https://data.london.gov.uk/dataset/london-atmospheric-emissions-inventory--laei--2016>  
628 (accessed 3.27.21).

629 Yan, Y., Pozzer, A., Ojha, N., Lin, J., Lelieveld, J., 2018. Analysis of European ozone trends in the  
630 period 1995–2014. *Atmos. Chem. Phys.* 18, 5589–5605. <https://doi.org/10.5194/acp-18-5589-2018>

631 Zhou, L., Liu, Q., Lee, B.P., Chan, C.K., Hallquist, Å.M., Sjödin, Å., Jerksjö, M., Salberg, H.,  
632 Wängberg, I., Hallquist, M., Salvador, C.M., Gaita, S.M., Mellqvist, J., 2020. A transition of  
633 atmospheric emissions of particles and gases from on-road heavy-duty trucks. *Atmos. Chem.*  
634 *Phys.* 20, 1701–1722. <https://doi.org/10.5194/acp-20-1701-2020>

635  
636  
637  
638



639 **Tables**

640

641 **Table 1.** Details of the sites and datasets used in this study.

City	Site	Type	Variables	Period
Copenhagen	Jagtvej	Street canyon	NO <sub>x</sub> , NO <sub>2</sub> , TR, VS	1994-2017
	H.C. Ørsted	Urban background	NO <sub>x</sub> , NO <sub>2</sub> , O <sub>3</sub>	
	H.C. Ørsted	Meteorology	T, RH, WS, WD	
London	Marylebone Road	Street canyon	NO <sub>x</sub> , NO <sub>2</sub> , TR, VS	1998-2017
	North Kensington	Urban background	NO <sub>x</sub> , NO <sub>2</sub> , O <sub>3</sub>	
	Heathrow	Meteorology	T, RH, P, WS, WD	
Stockholm	Hornsgatan	Street canyon	NO <sub>x</sub> , NO <sub>2</sub> , TR, VS	1992-2017
	Torkel	Urban background	NO <sub>x</sub> , NO <sub>2</sub> , O <sub>3</sub>	
	Högdalen	Meteorology	T, P, WS, WD	

642 T: air temperature, RH: relative humidity, WS: wind speed, WD: wind direction, P: atmospheric pressure

643

644

645

646

647

648

649

650

651

652

653

654

655

656

657

658

659

660 **Table 2.** Mean  $EF_{NO_x}$  and  $NO_2:NO_x$  emission ratios for several vehicle categories, taken from remote sensing  
661 studies conducted in European cities (UK: Carslaw et al., 2011; Carslaw and Rhys-Tyler, 2013; Carslaw et al.,  
662 2019; Ghaffarpasand et al., 2020, and Sweden: Liu et al., 2019; Zhou et al., 2020).

663

Variable	Euro stage	PC gasoline	PC diesel	LCV diesel	Truck (<12 t) diesel	Truck (>12 t) diesel	<sup>a</sup> Urban bus diesel
$EF_{NO_x}$ [g km <sup>-1</sup> veh <sup>-1</sup> ]	E0	2.38	1.22	1.46	5.36	<sup>b</sup> n.a.	n.a.
	E1	1.59	1.24	2.27	3.44	n.a.	11.13
	E2	1.05	1.30	2.01	5.95	13.01	12.35
	E3	0.41	1.23	1.83	5.33	10.61	15.58
	E4	0.23	1.00	1.57	5.09	7.75	16.93
	E5	0.14	1.02	1.86	5.33	7.59	12.78
	E6	0.19	0.51	0.67	2.64	0.74	2.40
$NO_2:NO_x$ [vol. %]	E0	3.2	10.8	7.6	6.2	n.a.	n.a.
	E1	2.8	16.8	12.5	11.0	n.a.	11.0
	E2	3.1	8.1	8.4	21.0	11.7	15.4
	E3	4.1	14.9	13.2	12.3	15.8	8.9
	E4	5.6	22.5	23.0	6.2	2.9	8.0
	E5	8.4	18.8	15.5	6.4	4.9	11.3
	E6	10.5	21.7	24.2	15.2	22.5	17.9

664 <sup>a</sup>A large variation could be observed within the same Euro stage, depending on the after-treatment system (Table S2,  
665 Supplementary Material). <sup>b</sup>Not available.

666  
667  
668  
669  
670  
671  
672  
673  
674  
675  
676  
677  
678  
679  
680  
681  
682  
683  
684

685 **Figure captions**

686

687 **Figure 1.** Monthly mean NO<sub>x</sub> and NO<sub>2</sub> concentrations at curbside and urban background sites (a-f), together with  
688 NO<sub>x</sub> and NO<sub>2</sub> street increment concentrations (g-l). The orange lines represent the meteorology-normalized  
689 concentrations. Note the different y-axis scales adopted to enhance the features in the time series of each site.

690

691 **Figure 2.** Yearly trends (bar plots; in  $\mu\text{g m}^{-3} \text{ yr}^{-1}$ ) and relative changes (numbers; in  $\% \text{ yr}^{-1}$ ) in NO<sub>x</sub> (a) and NO<sub>2</sub>  
692 (b) concentrations for the three cities over the period 1998-2017, based on monthly mean changes in  
693 meteorologically normalized air pollutant concentrations at urban background and curbside sites, together with  
694 street increments. The error bars show the 95% confidence intervals of the trends. \*Indicates that the trend is not  
695 significant.

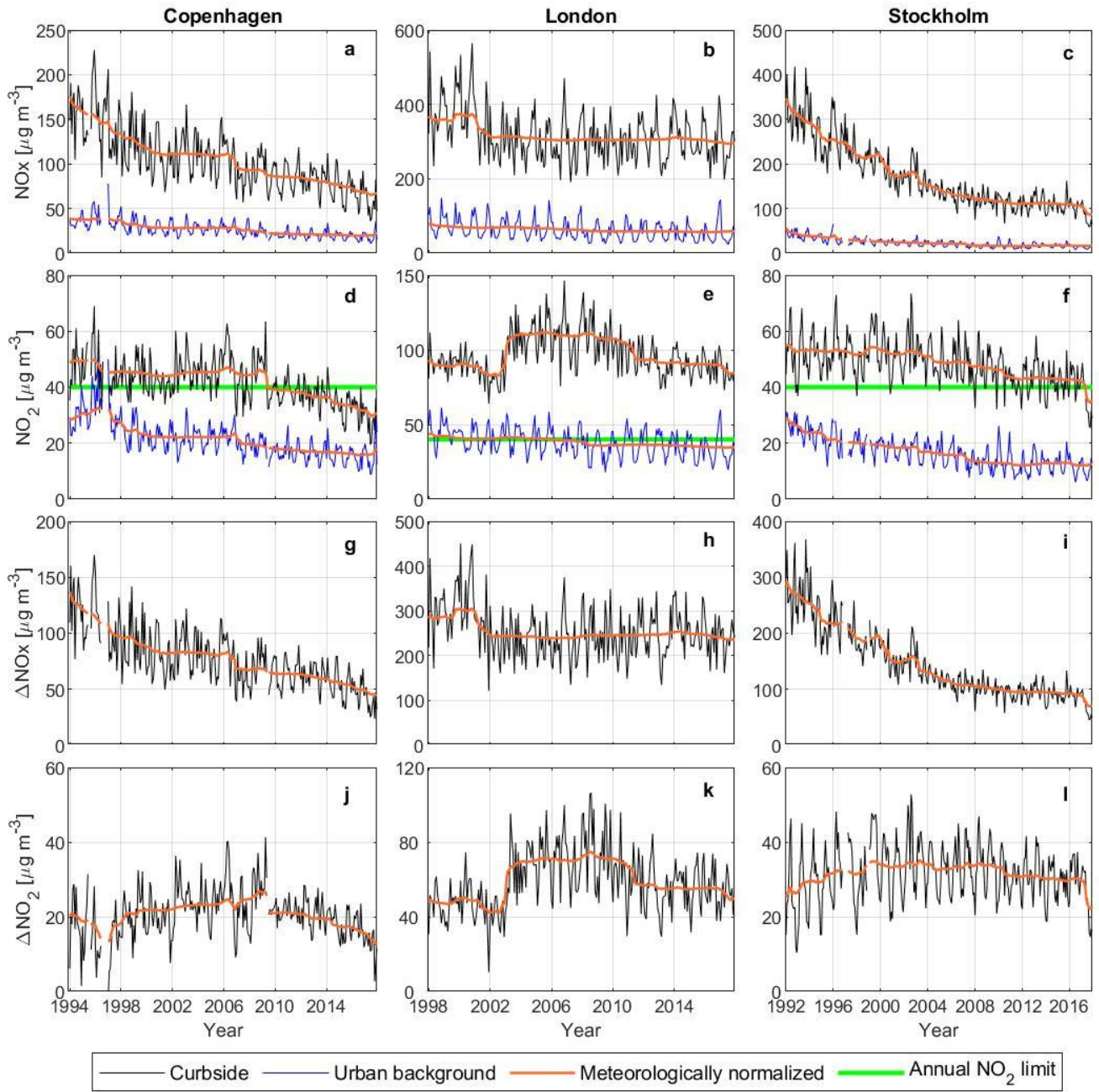
696

697 **Figure 3.** a-c) Annual mean EF<sub>NO<sub>x</sub></sub> for the vehicle fleet at the curbside sites, with the grey shadows representing  
698 the 95% confidence intervals. d-f) Annual mean  $\Delta\text{NO}_x$  concentrations (normalized) at curbside, together with the  
699 95% confidence intervals. g-h) Annual NO<sub>2</sub>:NO<sub>x</sub> emission ratios at curbside with 95% confidence intervals. j-l)  
700 Diesel PC penetration in the national markets (International Council on Clean Transportation, 2018) expressed as  
701 percentages of all PC (thick black line) and new PC (thin black line), together with Euro standard registration dates  
702 (E1: Euro 1, E6: Euro 6).

703

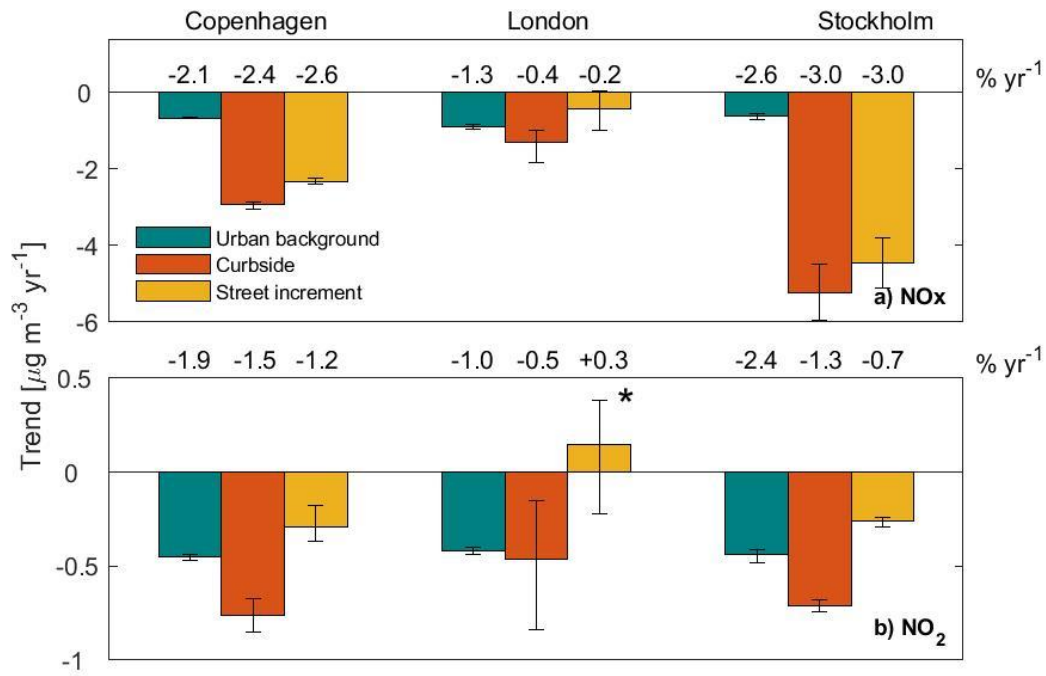
704 **Figure 4.** EF<sub>NO<sub>x</sub></sub> for the vehicle fleet at Hornsgatan site in the years 2009 and 2017 calculated using databases  
705 (EMEP and HBEFA), remote sensing studies (Table 2) and by inverse modeling. The error bars represent the 95%  
706 confidence intervals of the mean.

707



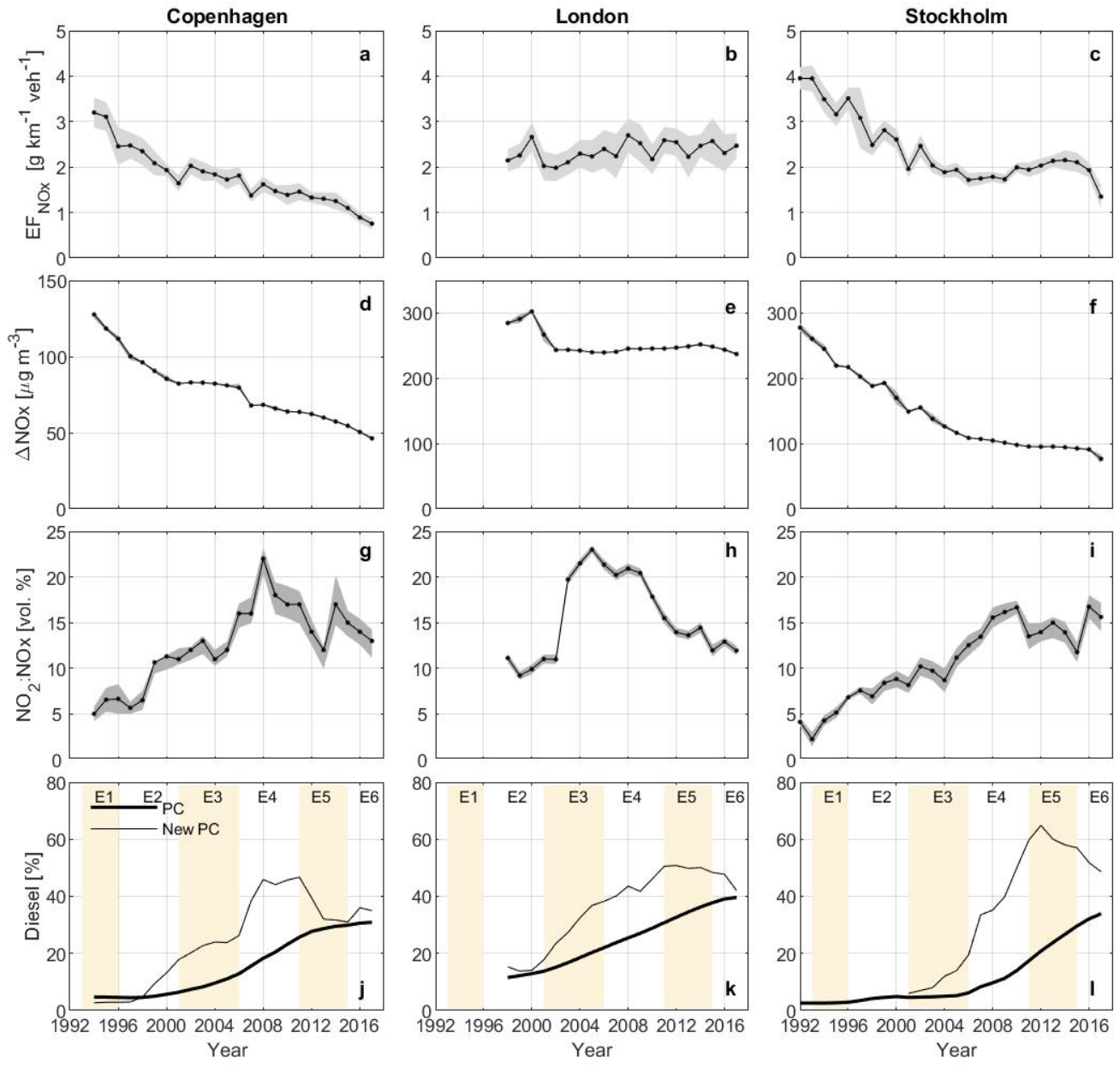
708  
709

**Figure 1**

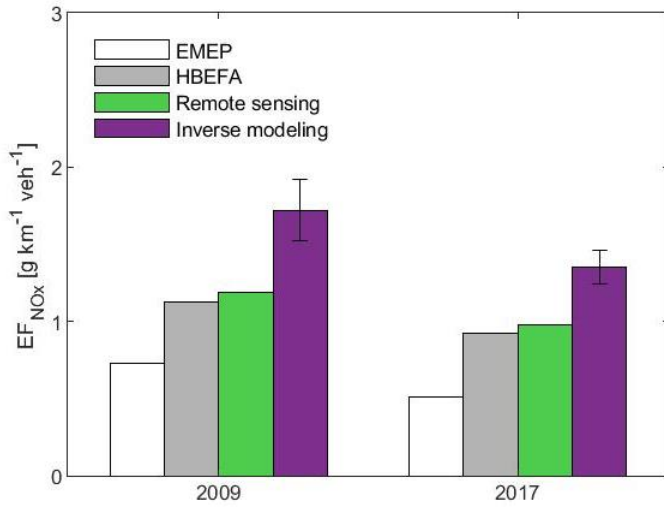


710  
711  
712

**Figure 2**



713  
714 **Figure 3**



715  
716 **Figure 4**